

## Surface temperature and salinity variations between Tasmania and Antarctica, 1993–1999

Alexis Chaigneau and Rosemary Morrow

Laboratoire des Etudes Géophysiques et Océanographiques Spatiales, Toulouse, France

Received 25 January 2001; revised 1 October 2001; accepted 24 October 2001; published 31 December 2002.

[1] Continuous surface temperature and salinity measurements have been collected onboard a supply ship between Tasmania and Dumont D'Urville, Antarctica, as part of the SURVOSTRAL program (Surveillance de l'Océan Austral). The ship makes 6–10 repeat sections per year from October to March for the period 1993–1999, and these measurements form the longest time series of spring and summer variations available in the Southern Ocean. The surface fronts are more clearly indicated with the salinity data than the temperature data. The Levitus climatological and Reynolds satellite monthly mean sea surface temperature data compare well with our surface temperature data: All data sets are dominated by the large-scale seasonal heating cycle with similar amplitude and phase. The SURVOSTRAL monthly mean sea surface salinity data show weak seasonal variations, except in the Antarctic Continental Zone where seasonal sea-ice variations introduce large surface freshwater fluctuations. The Levitus climatological surface salinity has too much seasonal variability and fails to reproduce the sharp fronts, the near-constant salinity in the Antarctic Zone, and the seasonal freshening near Antarctica. This has important consequences for projects that use Levitus climatology data to establish the surface salinity structure and water mass characteristics. *INDEX TERMS:* 4207 Oceanography: General: Arctic and Antarctic oceanography; 4215 Oceanography: General: Climate and interannual variability (3309); 4528 Oceanography: Physical: Fronts and jets

**Citation:** Chaigneau, A., and R. Morrow, Surface temperature and salinity variations between Tasmania and Antarctica, 1993–1999, *J. Geophys. Res.*, 107(C12), 8020, doi:10.1029/2001JC000808, 2002.

### 1. Introduction

[2] The Southern Ocean, due to its distinct geography, provides an important link by which water masses can be exchanged between the three major ocean basins. The major current in the Southern Ocean is the Antarctic Circumpolar Current (ACC), composed of a series of deeply penetrating fronts and strong jets which form the barrier that isolates the warm stratified subtropical waters from the more homogeneous cold polar water. The Southern Ocean is also one of the major site for the formation of the world's deep water masses. In the northern section around the Subtropical Front, central water is subducted and ventilates the subtropical thermocline in the Southern Hemisphere. Sub-Antarctic Mode Water (SAMW) is formed in the thick winter mixed-layers directly north of the Subantarctic Front [Mc Cartney, 1982]; the densest mode water formed is Antarctic Intermediate Water (AAIW). Closer to the continent, Antarctic Bottom Water (AABW) is formed in winter from the complex interactions between the ocean, atmosphere, and sea-ice. The resulting intense three-dimensional circulation also plays a role in the uplift of Circumpolar Deep Water (CDW) to intermediate levels via a complex redistribution throughout the three other ocean basins [Sloyan and Rintoul, 2001].

[3] The surface temperature and salinity in these regions of water mass formation are a critical factor in characterizing the different deep water masses, since these tracers are conserved when they are no longer in contact with the surface layer, although mixing can induce diffusive flux divergences that can alter the temperature and salinity of a fluid parcel. There is a marked surface density gradient across the ACC, with temperatures dropping by 10°C over 10 degrees latitude, partly compensated by a salinity decrease by 1.0 pss. In the Antarctic regions south of the ACC, there is no permanent thermocline and temperature remains fairly constant below the seasonal thermocline. Thus salinity becomes a key factor in the dynamics of the polar oceans. The surface layer salinity responds directly to the large variations in evaporation (in regions of strong wind-forcing, for example) and precipitation. Brine rejection from sea-ice formation in autumn and winter combined with very low temperature water over the continental shelf, can produce convective overturning to deeper layers (a key factor in the formation of AABW). The salinity distribution is also affected by the strong wind driven Ekman flux, which acts to transport and redistribute meridionally both the sea ice and its meltwater and creates a surface freshwater cap during spring-summer.

[4] The base of this fresh water cap is marked by an upper ocean halocline [Toole, 1981] that has important consequences for the vertical stability in the polar zone,

since the salinity stratification defines the limit for the upper mixed layer. Various climate models have shown in the Southern Ocean, that relatively minor changes in the surface heat and freshwater fluxes can have a dramatic effect on the salinity stratification. Increases in the surface freshwater input increases the salinity stratification and surface heat storage, and can eventually shut off the formation of AABW [Manabe and Stouffer, 1996; Sarmiento *et al.*, 1998]. Decreasing the freshwater fluxes can erode the halocline, allowing heat to penetrate more deeply, which leads to a rapid cooling of the upper ocean and the atmospheric circulation above [Gordon, 1991; Glowienka-Hense, 1995]. These consequences are so dramatic because of the weak stratification, and which means that a large volume of deep water can be influenced by the air-sea heat and salt exchange.

[5] Despite the importance of understanding the salinity budget in the Southern Ocean, long term measurements of even the upper ocean water mass characteristics are sparse. The WOCE (World Ocean Circulation Experiment) program over the last decade has brought an increase in the number of full repeat hydrographic sections across the ACC (see Rintoul *et al.* [1999] for a review), though these sections are at best, once or twice per year. A number of repeat XBT lines provide more frequent temperature measurements across the ACC near Drake Passage (Janet Sprinall, personal communication), south of Tasmania [Rintoul *et al.*, 1997], and south of New Zealand [Russo *et al.*, 1999]. But long term salinity monitoring is almost nonexistent.

[6] In this paper, we present the first results from a program of long-term monitoring of the sea surface temperature (SST) and salinity (SSS) characteristics across the ACC in the region south of Tasmania. Seven years of thermosalinograph data have been collected as part of the SURVOSTRAL program (Surveillance de l'Océan Austral), an international collaboration between Australia, France and USA established in 1992 to monitor the upper ocean variations across the ACC [Rintoul *et al.*, 1997]. The SURVOSTRAL line crosses the ACC in a region of growing eddy energy [Morrow *et al.*, 1994] (R. A. Morrow *et al.*, Seasonal and interannual variations of the upper ocean energetics between Tasmania and Antarctica, submitted to *Deep Sea Research*, 2001, hereinafter referred to as Morrow *et al.*, submitted manuscript, 2001), where the ACC is constrained to pass over the Southeast Indian Ridge before turning to the southeast and entering the deeper and eddy-rich Tasman Basin, and finally encountering the Macquarie Ridge choke point (see Figure 1). These bathymetric constraints introduce strong spatial gradients in the flow dynamics. The high-resolution surface temperature and salinity data are only available over the spring and austral summer from late October to early March, but they allow us to calculate the monthly means over these five months, and also establish the interannual variations of the summer warming cycle over the 7 year period.

[7] In section 2 we describe the data processing for the thermosalinograph data. In section 3, we consider whether the ACC fronts can be monitored simply by the surface temperature and salinity characteristics, by examining their relation with the subsurface fronts located from XBT data. In section 4 we present the summer monthly mean surface temperature and salinity structure at fine resolution along

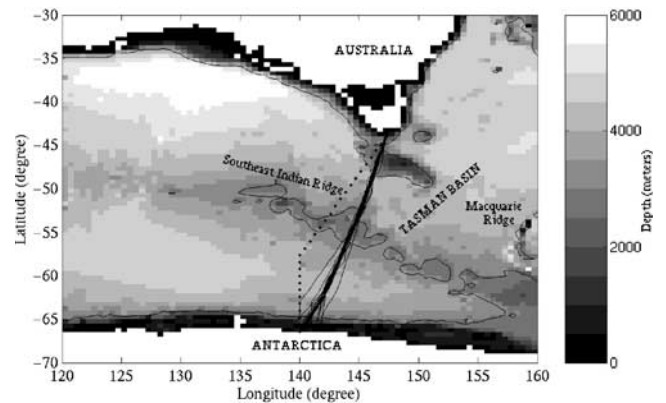


**Figure 1.** ASTROLABE transects retained in our analysis from 1993 to 1999 (solid lines). The WOCE SR3 line is also marked (dotted line). The 3000 m depth contour is marked.

the SURVOSTRAL line, and compare our results with the Levitus [1998] climatological data and Reynolds SST fields interpolated onto the SURVOSTRAL line. In section 5 we consider the temperature and salinity anomalies with respect to the average summer cycle over the 5 year period, 1993–1997. Unfortunately the salinity calibration data was lost for the period November 1997 to the end of 1999, which effectively reduces our calibrated salinity time series. We also investigate how the surface salinity in the polar zone responds to changes in the sea-ice coverage, as measured by the ERS satellite.

## 2. Thermosalinograph Data

[8] The data was collected as part of the SURVOSTRAL program, providing continuous measurements of surface temperature and salinity from the thermosalinograph of the French Antarctic supply ship, the *Astrolabe*, with XBT measurements to 800 m taken every 30 km. The measurements are made 6 times a year from October to March, on a nearly repeating line from Hobart (43°S, 147.5°E) to the French Antarctic base, Dumont D'Urville in Adélie Land (66°S, 140°E). Analysis of the XBT data is discussed in separate publications [Rintoul *et al.*, 1997, 1999] (Morrow *et al.*, submitted manuscript, 2001).

[9] The thermosalinograph sensor is mounted in the *Astrolabe's* seawater intake pipe. Seawater is pumped in from the bow intake, to minimize pollutants and mixing by the ship's passage. The temperature and conductivity are averaged over a 5 minute interval, giving about one measurement every nautical mile (1.85 km), depending on the ship's speed. The data were first checked for errors, which are principally due to problems with the update of the GPS positioning, anomalous values around the northern end as we leave the Hobart port, and salinity spikes, mainly a sudden lowering of salinity which could either be due to a local storm, or the presence of air bubbles in the thermosalinograph intake. Obvious errors from the first two problems were removed. The spiking problem, being predominantly in one direction (low salinity), was minimized by applying a median alongtrack filter to smooth the data. Since we are mainly concerned with the seasonal and interannual changes

on Rossby radius space scales, the 5' alongtrack values were first smoothed with a 9-point median filter to reduce the spiking problem. The alongtrack data was then interpolated onto a fixed 0.05° latitude grid (5.5 km).

[10] In order to calculate temporal variations along the mean SURVOSTRAL path, and because we are in an inhomogeneous region with strong geographical variations (especially on the frontal zone), we applied strict limits on the definition of a «repeating track». Any data that was more than 2° longitude from the mean path was eliminated from the analysis, which removed 14 tracks from the available 44 over the period October 1993 to December 1999. Figure 1 shows that the remaining tracks are tightly grouped in the high energetic frontal zone (north of 54°S) with slightly wider spacing between transects in the Antarctic zone (south of 55°S) which has more uniform characteristics (see section 3). Unfortunately, this technique consistently removed data from the October/November period, when the spring sea-ice coverage was still important, and the ship moved offtrack to find the biggest leads through the sea-ice.

[11] The final step was to calibrate the salinity values. Surface salinity samples were collected onboard from the same seawater intake once per day, giving 6 bottle samples per section. These bottle samples were analyzed on a Guildline Autosal at CSIRO, Australia, with an estimated accuracy of  $\pm 0.003$  pss. In addition to the low spiking problem, the thermosalinograph data were consistently lower than the calibration data. To correct for this, we adjusted the thermosalinograph SSS along each transect by the mean difference between the bottle samples and the collocated SSS. Unfortunately, the calibration data from November 1997 to the end of 1999 were lost, and so our seasonal salinity analysis is based only on the years 1993–1997. The temperature sensor is calibrated at the start of each season. We estimate the precision of the SST as  $\pm 0.01^\circ\text{C}$  based on the standard deviation of the 10 second data used in each 5' average. The SSS precision of  $\pm 0.02$  pss is estimated as the mean difference between neighboring SSS values, outside regions with strong gradients.

### 3. Fronts

[12] The Antarctic Circumpolar Current is actually composed of a series of sharp temperature and salinity fronts, which separate the subtropical and subpolar water masses. The strongest currents are associated with the sharpest density gradients. In the region south of Tasmania, these fronts are fairly tightly grouped, due to the presence of bathymetric ridges to the north and south. The frontal positions are generally defined by their subsurface temperature structure, and there exists a variety of definitions (see *Belkin and Gordon* [1996] for a review). In this study, we have retained the following subsurface definitions:

1. Subtropical Front (STF): Location of the 11°C isotherm at 150 m depth [*Nagata et al.*, 1988]. The temperature and salinity gradients of the STF are limited to the upper few hundred meters and are nearly density-compensating, so the transport associated with the front is small (S. Sokolov and S. R. Rintoul, Structure of Southern Ocean fronts at 140°E, submitted to *Journal of Marine Systems*, 2001a, hereinafter referred to as Sokolov and

Rintoul, submitted manuscript, 2001a). This front, centered around 45–46°S separates the Subtropical and the Subantarctic Zones.

2. Subantarctic Front (SAF): Maximum temperature gradient between 3 and 8 °C at 300 m depth [*Belkin*, 1990]. At the WOCE SR3 line, Sokolov and Rintoul (submitted manuscript, 2001a) find two distinct branches for the SAF; in our region, multiple filaments occur more rarely (only 5 of our 32 sections showed two branches). The SAF centered around 51°S forms the limit between the Subantarctic and Polar Frontal Zones.

3. Polar Front (PF): Northern limit of temperatures cooler than 2°C at 200 m depth [*Botnikov*, 1963]. South of this front centered at 53–54°S, we have the more homogeneous water properties in the Antarctic Zone.

4. Southern ACC Front (SACCF): *Orsi et al.* [1995] found that the SACCF usually coincided with the southern limit of the 1.8°C isotherm water of the Upper Circumpolar Deep Water at depths greater than 500m. The SACCF is found around 61°S and separates the Antarctic and the Continental Antarctic Zones.

[13] Although defined at depth, these fronts also have surface expressions, and previous studies have used the surface characteristics to study the location of the Polar Fronts, such as *Moore et al.* [1999] using the SST signal for the PF, and *Gille* [1994] who used altimetric sea level anomalies to study the SAF and PF. In this section, we will examine how well the surface thermosalinograph fronts match up with the subsurface temperature fronts from XBT data, using the first three frontal positions defined above. The description for the processing of the concurrent XBT data is given by *Rintoul et al.* [1997] and Morrow et al. (submitted manuscript, 2001). Our definition of the surface fronts is based mainly on the SSS gradients [*Chaigneau*, 2000], and is as follows:

1. STF: Its surface signature is identified as the maximum SSS gradient occurring within the latitude range 44.5–47°S, and which has a corresponding signature in SST.

2. SAF: As for the STF, but within the latitude range 49–52°S.

3. PF: The surface signature of the PF is taken as the northern limit of a region of near constant SSS around 33.85 pss, often coinciding with a local SSS minimum and a SST gradient.

[14] We find that the SST signature does show temperature steps around the position of the subsurface temperature fronts. However, these are of similar magnitude to the mesoscale eddy signal, and it is quite easy to misplace them. The SSS clearly shows three main steps in salinity, with salinity gradients of around 0.5 pss over 50 km distance.

[15] As an example, Figure 2 shows the thermosalinograph SST and SSS, and the subsurface temperature structure from XBT data, for a section between Tasmania and Dumont D'Urville for the period 29 December 1993 to 3 January 1994. The position of the three subsurface fronts is marked on the surface plots and on the XBT profile. For this transect, the surface position of the PF and STF are about 1° north of the subsurface definition. When the same calculation is repeated for all transects from 1993 to 1997 [*Chaigneau*, 2000], we find that the mean surface STF, SAF and PF are generally further north (0.21°, 0.14°, 0.72° respectively) than their subsurface counterparts. However,

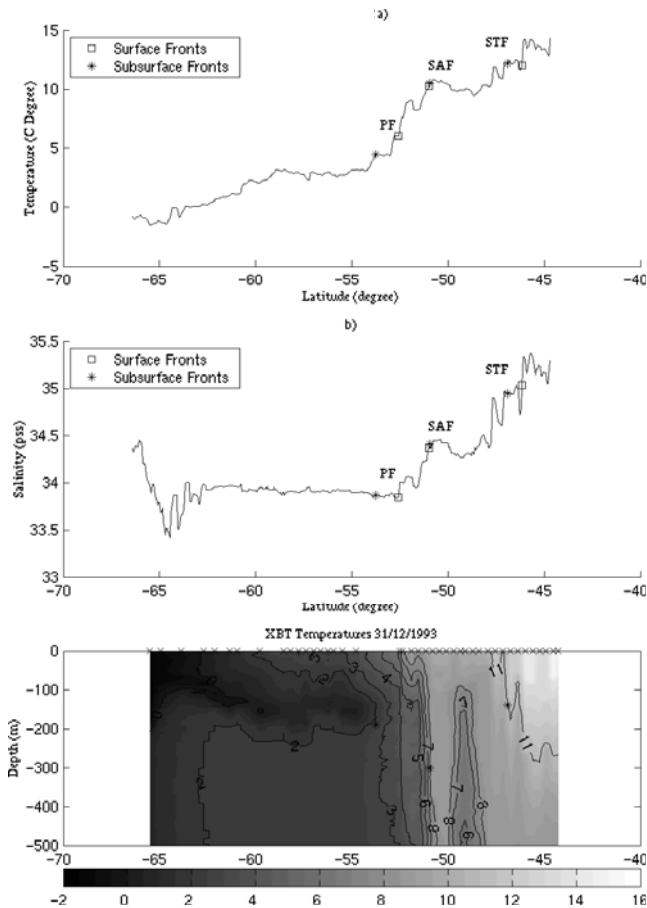


**Figure 2.** a) Thermosalinograph SST and b) SSS and c) the subsurface temperature structure from XBTs, for a section between Tasmania and Dumont D’Urville for the period 29 December 1993 to 3 January 1994. The surface front positions are marked in a) and b); the subsurface front positions are marked on all plots.

there is a large standard deviation associated with this calculation (0.39°, 0.40°, 0.69° respectively) due to high mesoscale activity and multiple filaments associated with these fronts. We can say that with an error of 0.5° latitude, the surface SSS gradients do give indications of the subsurface frontal positions.

**4. Summer Monthly Variations**

[16] With the thermosalinograph data interpolated onto a fixed latitude grid, we have calculated the monthly averaged SST and SSS profiles between Hobart and Antarctica, from November to March for the period 1993 to 1997. Table 1 shows the number of transects available during this period for each month—note that the monthly mean values for January–February have the most profiles along the mean XBT path. The single late October transect and the two from early November, are grouped together to calculate the monthly mean of November.

**4.1. Temperature Structure**

[17] Figures 3a–3e show the summer monthly mean SST profiles for November–March with their standard devia-

**Table 1.** Number of Thermosalinograph Sections Per Month Along the Mean SURVOSTRAL Line for the Period 1993–1997, and for the Period 1993–1999, Which Includes the Uncalibrated Salinity

Period	1993–1997	1993–1999
October	1	2
November	2	4
December	4	7
January	10	13
February	10	13
March	3	5
Total	30	44

tions calculated along SURVOSTRAL line. These are compared with the monthly means SST from the *Levitus* [1998] climatology and from Reynolds satellite data interpolated onto the SURVOSTRAL line. The temperature gradients across the fronts are much sharper in the higher resolution thermosalinograph data. However, the other two

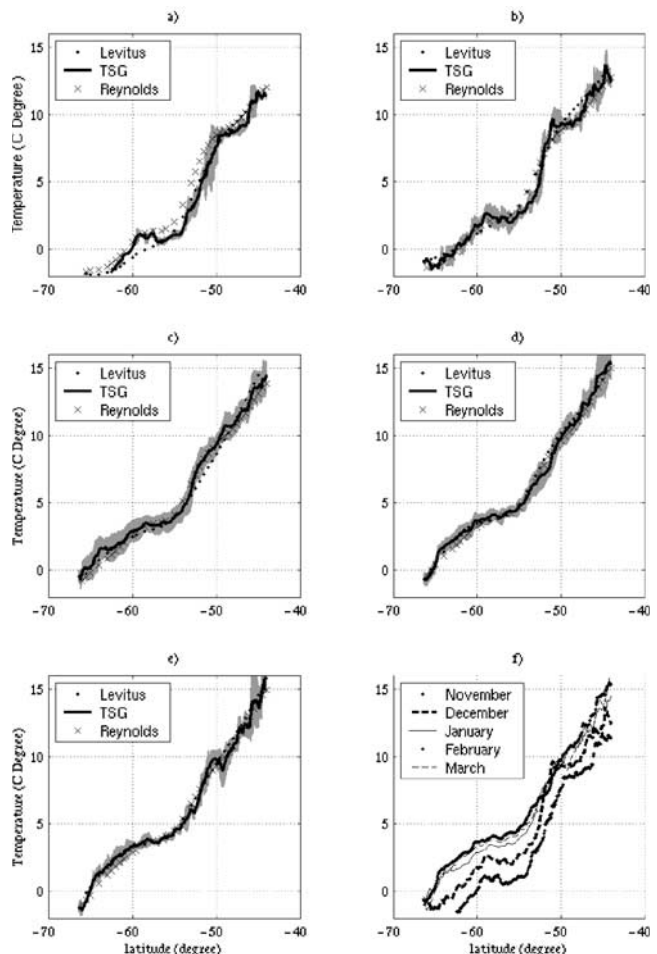


**Figure 3.** Summer monthly mean SST interpolated onto the mean SURVOSTRAL line from the *Levitus* [1998] climatology, Reynolds satellite data and the thermosalinograph data, for the period 1993–1997. Figures a) to e) show each monthly average from November to March. The standard deviations associated with the thermosalinograph SST are shaded in gray. Figure f) shows the 5 monthly curves superimposed.

data sets are generally within one standard deviation of our mean value. Figure 3f shows the ensemble of monthly thermosalinograph SST measurements; the main trend is the summer heating cycle which raises the temperature along the entire track by 2–3 °C. This warming cycle is also well captured by the Reynolds satellite data and Levitus climatology. The lowest temperatures are in austral spring (November–December) with a consistent increase in temperature to a maximum in February, then slight cooling along the entire track in March.

#### 4.2. Salinity Structure

[18] The thermosalinograph salinity data shows more striking differences (Figure 4). First, the summer variation is much less marked (Figure 4f)—the salinity curves are tightly grouped from November to March, unlike the climatological SSS. The exception is close to the Antarctic continent, near 64–65°S, where the sharp surface salinity minimum of 33.5 in December is gradually eroded to 33.6 in January, 33.8 in February and 33.85 in March. This salinity minimum reflects the input of surface freshwater during the spring sea-ice melt. As summer progresses, there is less available sea-ice in the surface layer and continued mixing with the underlying saltier waters can increase the surface salinity. In the *Levitus* [1998] climatological data, this SSS minimum is not apparent or is found further north (in January the salinity minimum is at 57°S!).

[19] In the Antarctic Continental Zone south of 65°S, there is also a consistent salinity increase to values greater than 34.0 in January to March. Again, this feature is not well captured by the climatological data. This region is one of extremely cold surface waters (monthly mean values of –0.5 to –1.5 °C in summer) and could indicate the lingering trace of brine rejection from sea-ice formation (which extends on average to 62°S in August/September). Another cause could be increased vertical mixing with the saltier deeper layers as we approach the shallower coastal region.

[20] In the Antarctic Zone further north (54–61°S), the measured SSS shows a minor freshening, from 34 at 62°S to 33.8 at 53°S in November/December. The Antarctic Divergence is strongest from 60–64°, which leads to upwelling of more saline Upper Circumpolar Deep Water (UCDW) to the base of the mixed layer and may increase the SSS at 60°S. As summer progresses, this local maximum in SSS decreases to a more constant  $33.84 \pm 0.02$  pss as the thermal stratification sets in.

[21] In the climatological data, the large salinity variations greater than one standard deviation from our mean are probably influenced by the sparse salinity data. For example, the monthly climatological SSS maps (not shown) indicate that the minimum of 33.6 pss at 57°S in January is caused by a lens of low salinity water crossing the SURVOSTRAL line. This lens is not evident in the *Levitus* 94 data set and its origin is unknown, as it is not evident in the adjacent WOCE campaigns in 1995–1997 (S. R. Rintoul, personal communication). This example highlights that much of the high salinity variability in the 50–60°S zone may be influenced by a few individual observations, and underlines the lack of good spatial and temporal coverage in the 1998 climatological data sets.

[22] Further north in the Polar Frontal region, salinity is a clear indicator of the Southern Ocean fronts, with a change

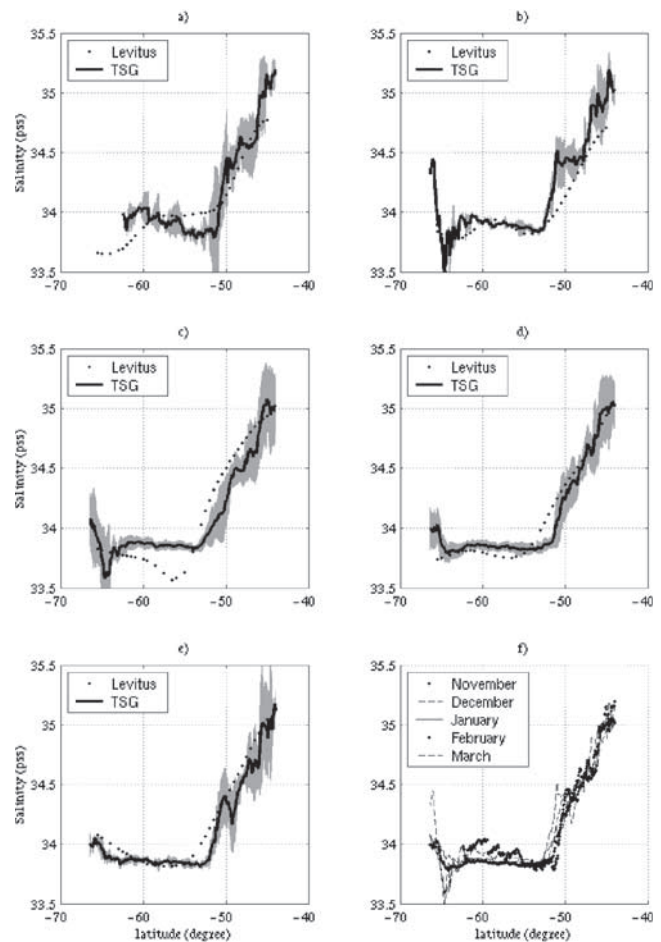


**Figure 4.** As for Figure 3, except for salinity data: thermosalinograph and *Levitus* [1998] climatology.

in meridional SSS gradient around 52–54°S marking the Polar Front, very sharp salinity gradients with SSS increasing from 33.8 to 34.4 associated with the Subantarctic Front around 50°S, and SSS increase from 34.6 to 35.0 associated with the Subtropical Front near 46°S. The monthly mean standard deviations have increased to 0.2 pss in this region connected to mesoscale displacements of the fronts which carry either subtropical water (warm and salty) to the south or cold, fresher water northward. Despite these large standard deviations, the oversmoothed *Levitus* SSS climatology remains more than one standard deviation outside our observed mean SSS profile.

#### 4.3. T,S Diagram

[23] The main surface T-S features can also be summarized by the summer monthly mean temperature-salinity diagrams along the SURVOSTRAL line, shown in Figure 5. We have marked the mean position of each of the surface fronts for each month to the discussion. The water mass characteristics of AABW and UCDW are also marked. Between the PF and the STF we have a near linear increase in temperature and salinity northward, although the temperature increase to the north is larger in summer (JFM) than in spring (ND). The seasonal differences are dominated by the seasonal heating cycle which is clearly evident in the

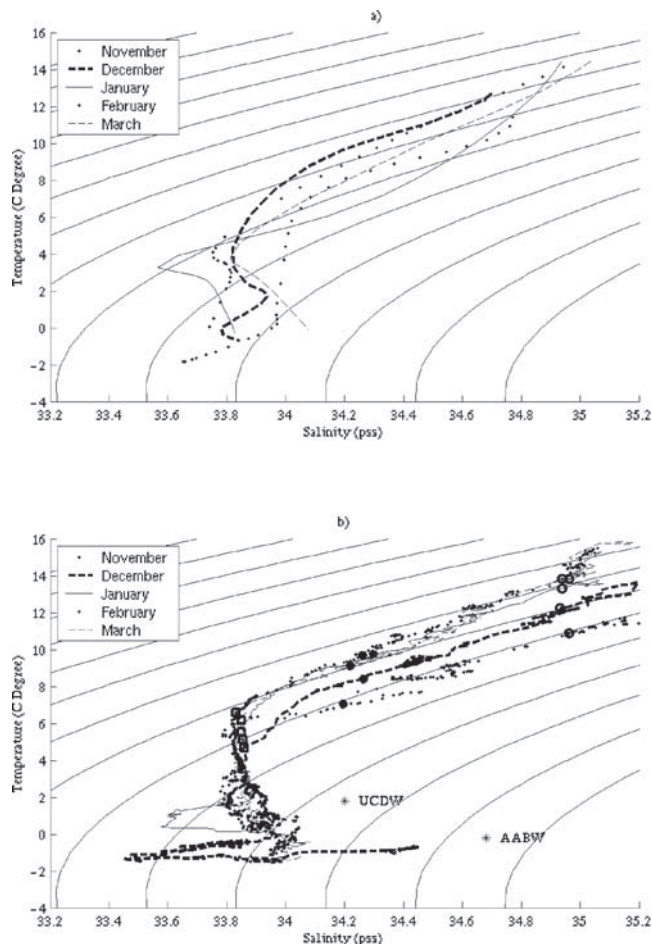


**Figure 5.** Summer monthly T,S diagrams from a) *Levitus* [1998] climatology and b) thermosalinograph data set. The potential density is superimposed (density range from 1024.75 to 1028 kg/m<sup>3</sup> with contour interval of 0.25 kg/m<sup>3</sup>). The monthly mean position of the polar fronts are marked: PF—square; SAF—dot; STF—circle. The temperature and salinity characteristics of AABW and UCDW are shown.

vertical temperature shifts of the PF and the STF. The surface density changes more rapidly south of the PF. As the temperature decreases southward, the salinity shows a minor increase in the direction of mixing with UCDW. The December salinity minimum of 33.45 ps at  $-1.3^{\circ}\text{C}$  indicates sea-ice melt; this lens of surface water warms and becomes more salty in January although the water mass remains on the same isopycnal. By February/March, this fresh surface layer has been warmed and mixed with the saltier underlying UCDW. Close to the coast at temperatures less than  $1^{\circ}\text{C}$ , the increase in salinity is in the direction of mixing with Antarctic Shelf Water made salty as a result of brine rejection.

[24] The climatological surface T-S relationship shows similar trends north of the Polar Front. However, there is too much seasonal variation in the salinity which would imply more diapycnal mixing or air-sea fluxes than is evident in the thermosalinograph data. The most glaring differences are south of the Polar Front. The Levitus January salinity minimum occurs at  $57^{\circ}\text{S}$  where the surface water is

warmer than  $3^{\circ}\text{C}$ ; in the SURVOSTRAL data the minimum SSS occurs at a temperature below  $1^{\circ}\text{C}$  and forms a denser water mass. The Levitus November surface properties are too salty and too dense, remaining at 34.0 rather than 33.8 ps. The increase in SURVOSTRAL salinity near Antarctica occurs only in waters cooler than  $1^{\circ}\text{C}$ : *Levitus* [1998] shows the salinity increase with waters of  $4^{\circ}\text{C}$  in January and March. The climatology data shows only a minor fresh surface water signal close to the coast during summer, which means the surface layers are too salty and dense which will influence the stability of these surface water masses. Finally we note that the climatological SST and SSS measurements which extend to the continent at  $66^{\circ}\text{S}$  in spring are probably based on very few data points since the average sea-ice coverage extends to  $63.1^{\circ}\text{S}$  during November.

## 5. Interannual Variations of Summertime SST and SSS

[25] The thermosalinograph data allows us to examine the interannual changes over the summer months in surface temperature and salinity at the SURVOSTRAL longitude. We first remove the summer monthly mean values calculated over the 4 year period 1993–1997 at each point along the line. The 4 year mean is used since we have the problem of uncalibrated salinity data for the period November 1997 to 1999. To extend our interannual SSS series over the interesting El Niño period, these uncalibrated SSS data were adjusted as follows: we first calculated the SSS mean over the homogeneous  $54\text{--}60^{\circ}\text{S}$  zone, during the 1993–1997 period (value of 33.825 ps). We then calculated the mean of each uncalibrated transect over the same region, and adjusted the entire transect by the difference (mean-33.825 ps).

[26] Figures 6a, 6b, and 6c show Hovmuller diagrams of the Reynolds SST, SURVOSTRAL temperature and salinity anomalies, respectively. In the frontal zone north of  $54^{\circ}\text{S}$ , the thermosalinograph data are characterized by small scale anomalies, with spatial scales of 100–300 km alongtrack, and timescales of one to three months. This region is highly energetic, and the anomalies represent both transient eddies and longer period meanders (Morrow et al., submitted manuscript, 2001). These temperature and salinity anomalies are strongly correlated and correspond to meanders or eddies moving cool fresher water northward, or warm saltier water southward, across the mean seasonal position of each front. In the Antarctic Zone from  $54^{\circ}\text{S}$  to  $61^{\circ}\text{S}$ , the temperature and salinity anomalies are more large-scale, and these departures from the summer seasonal mean are likely to be directly modified by the atmospheric forcing, rather than responding to internal ocean dynamics. The interannual thermosalinograph temperature variations ( $\sim 3\text{--}5^{\circ}\text{C}$  in the frontal zone and  $1\text{--}2^{\circ}\text{C}$  in the Antarctic zone) are of comparable magnitude to the  $3\text{--}4^{\circ}\text{C}$  seasonal warming cycle (Figure 3f). Similarly, the seasonal cycle and the interannual SSS variations have similar magnitudes (0.4 ps in the frontal zones; 0.2 ps in the Antarctic Zone). Although the Reynolds SST satellite data captures the seasonal SST cycle quite well (Figures 3a–3e) and the phase of the interannual variations, the amplitude of the interannual signal is weaker than the thermosalinograph SST by  $0.5\text{--}1^{\circ}\text{C}$  (Figure 6a).

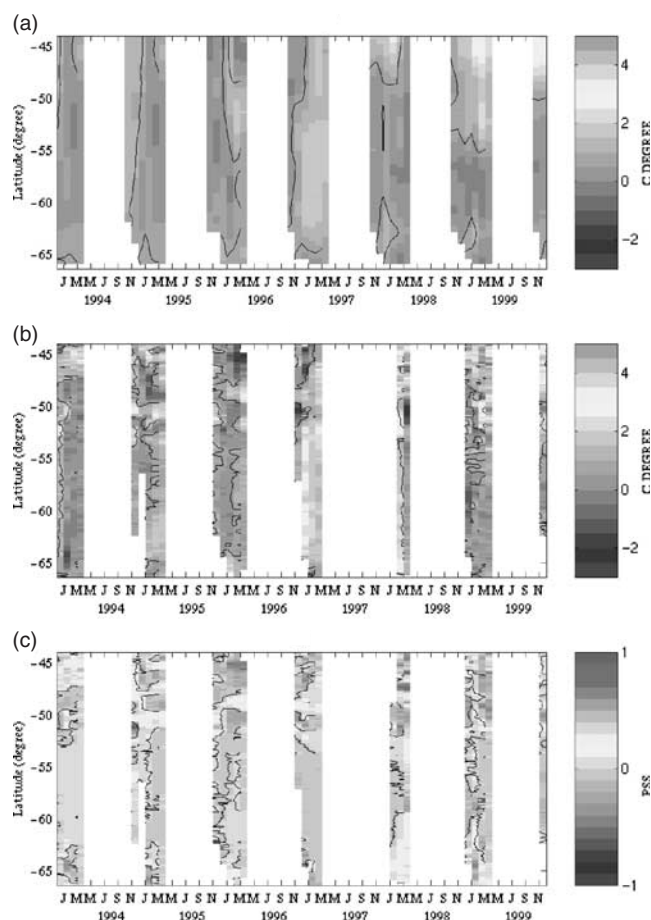


**Figure 6.** Hovmuller diagrams of a) Reynolds satellite SST anomalies, b) the thermosalinograph surface temperature anomalies. The monthly mean temperature calculated over the 1993–1997 period is removed at each point along the line. c) The thermosalinograph surface salinity anomalies are calculated relative to the mean period 1993 to 1997; values for 1988 and 1999 are adjusted but not calibrated (see text for details). See color version of this figure at back of this issue.

[27] The large-scale variations show four years of cooler than average temperatures (on average  $-0.5^{\circ}\text{C}$ ) in early 1994, 1995, 1996, 1999 with two years of warmer than average temperatures, in early 1997 and 1998. This confirms satellite SST analyses which indicate a large warming event in the Southern Ocean after the El-Niño of 1997 [Cabanes *et al.*, 2001], which is also in phase with the passage of the Antarctic Circumpolar Wave (ACW) with the northern section lagging the southern anomalies (S. Sokolov and S. R. Rintoul, The subsurface structure of interannual SST anomalies in the Southern Ocean, submitted to *Geophysical Research Letters*, 2001b). The salinity anomalies associated with this ACW signal are small—in the Antarctic Zone, salinities were only 0.05 pss higher in early 1994, and 0.05 pss lower in early 1997, and otherwise near zero. At the northern end of the transect, strong warm, salty anomalies becomes evident in early 1997, then strengthens to a maximum in 1998/1999 and continues through to early 2000. These warm salty anomalies could be influenced by a stronger southward extension of the East Australian

Current during the period (S. R. Rintoul, personal communication). Unfortunately, the uncalibrated salinity data in 1998/1999 stops us from making a profound analysis of the SSS over the interesting post-El Niño period.

[28] Between  $61^{\circ}\text{S}$  and  $66^{\circ}\text{S}$ , we have SST anomalies of less than  $1^{\circ}\text{C}$ , which are anticorrelated with the SSS anomalies of up to 0.4–0.5 pss. In this case, we have alternate years of cold, salty anomalies and warm, fresh anomalies. We have examined the sensitivity of annual ice area on our SSS signal. Although we expect SSS to vary in response to ice volume changes, the ice area and ice volume may be well correlated (if we assume the ice has similar thickness everywhere). Figure 7 shows the surface area anomaly of sea-ice coverage between  $120^{\circ}\text{E}$  and  $150^{\circ}\text{E}$ , as measured by the ERS scatterometer (taken as the measured backscatter coefficient at  $40^{\circ}$  incidence angle). This anomaly is calculated relative to the seasonal cycle of sea-ice coverage for this zone over the period 1993–1999. This area was chosen to include the downstream advection effects on the SURVOSTRAL SSS, but the results are robust even when we vary the width of the chosen zone.

[29] The mean salinity anomaly between  $61^{\circ}\text{S}$  and  $66^{\circ}\text{S}$  is superimposed in Figure 7. Maximum sea-ice extent occurs during the winters of 1994 and 1996. The sea ice melt introduces more freshwater input at the surface, and the following summer the SSS is lower than normal. The opposite occurs in the winter of 1993 and 1995: minimum sea-ice coverage, and higher surface salinities the following summer. The higher SST that occurs with lower salinities may be a result of the freshwater cap creating a surface barrier layer. The halocline underneath the barrier layer could block the downward penetration of summer heat, giving anomalous warming in the surface layer. Interestingly, the XBT temperature profiles show cooler anomalies during these events from 50 to 400 m. At this stage, without additional salinity data at depth, we can not determine whether these T,S variations are due to lateral frontal shifts, or the halocline blocking the downward penetration of heat, giving anomalously cool temperatures below. This discussion is not valid for the two last years (1998–1999) when the salinity is not calibrated.

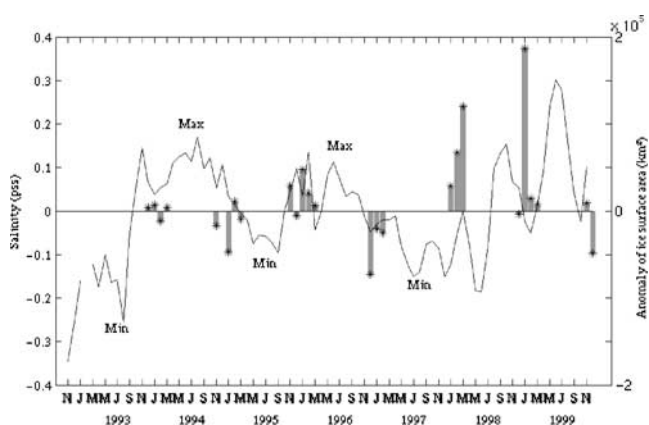


**Figure 7.** Time series of the surface area anomaly sea-ice coverage in the Antarctic region from  $120^{\circ}\text{E}$  and  $150^{\circ}\text{E}$  measured by the ERS satellite scatterometer (solid line). The mean surface salinity anomaly between  $61^{\circ}\text{S}$  and  $66^{\circ}\text{S}$  is superimposed (\*).

## 6. Conclusions

[30] Our analysis of thermosalinograph data south of Tasmania has quantified the strength and resiliency of the polar SSS fronts, and documented the spatially homogeneous SSS field in the Antarctic Zone (54–61°S). The size of the SSS gradients across the SAF and STF are estimated to be 0.5 pss, with a standard deviation of 0.2 pss. Large variability is chiefly due to the intense mesoscale variability across the fronts. The PF is clearly observed as the northern limit of the near homogeneous SSS in the Antarctic Zone; this zone has a mean SSS of 34.84 with a standard deviation of 0.02 pss.

[31] Are these results representative of the rest of the Southern Ocean? We have seen that the mean seasonal temperature structure is well represented by *Levitus* [1998] climatology, and the Reynolds SST product. Furthermore, the larger-scale interannual variations are well captured by the satellite SST product, although the amplitude is weaker. With little or no ship data at these latitudes, this is an encouraging validation of the climatological and satellite SST fields. We do note, however, that our limited regional study is actually relatively well sampled for the Southern Ocean. It has been the site of numerous hydrographic campaigns starting with Dumont D'Urville's summer campaign in 1840 [*Tchernia*, 1951a, 1951b], and fairly regular surveys in the 1930s, and every few years since the 1950s (see *Rintoul et al.* [1997] for a comprehensive review of previous hydrographic campaigns). So the climatological mean SST may be more robust than in other Southern Ocean locations.

[32] The amplitude of the SSS gradients across the SAF, and the near homogeneous SSS in the Antarctic Zone, are also observed during the 3 repeat summer sections at the WOCE SR3 line around 140°E (S. Rintoul, personal communication). The seasonal SSS variation over the November to March period is weak, except in the Antarctic Continental Zone where the sea ice melt creates a large seasonal freshwater flux at the surface. In contrast, the climatological data shows large seasonal variations that appear to be biased by individual salinity events and the large spatial averaging across the salinity gradients. This result is actually encouraging: future salinity measurements with a denser spatial coverage, for example from the ARGO profiling lagrangian drifter program, should provide a better mean salinity structure, without having to resolve the seasonal warming cycle. Complementary time series, such as the SURVOSTRAL line, will still be necessary to monitor biases and validate the interannual variations.

[33] **Acknowledgments.** We would like to thank the captain and crew onboard the *Astrolabe*, as well as our numerous volunteer observers, for helping us collect these measurements in the frequently inhospitable weather conditions. Special thanks to Steve Rintoul, Ann Gronell and Peter Jackson of CSIRO, Australia for their work in handling the logistics of the program, and the data preparation and quality control. Our thanks as well to Steve Rintoul, Gilles Reverdin, John Toole and our reviewers for early comments on the paper. The SURVOSTRAL program receives support from the Institut Français pour la Recherche et la Technologie Polaire (IFRTP), the PNEDC as part of the French CLIVAR program, the CSIRO Division of Oceanography's Climate Change Program, and the National Oceanic and Atmospheric Administration (NOAA-USA) through a cooperative agreement NA37GP0518. The Polar Sea-Ice grids of ERS were provided by the Department of Oceanography from Space, IFREMER, France.

## References

- Belkin, I. M., Hydrological fronts of the Indian Subantarctic, in *The Antarctic. The Committee Reports*, vol. 29, pp. 119–128, Nauka, Moscow, 1990 (in Russian with English abstract).
- Belkin, I. M., and A. L. Gordon, Southern Ocean fronts from the Greenwich Meridian to Tasmania, *J. Geophys. Res.*, **101**, 3675–3696, 1996.
- Botnikov, V. N., Geographical position of the Antarctic Convergence zone in the Southern Ocean, *Inf. Soviet Antarct. Exped.*, **41**, 324, 1963.
- Cabanes, C., A. Cazenave, and C. Le Provost, Sea level change from Topex-Poseidon altimetry for 1993–1999 and possible warming of the Southern Ocean, *Geophys. Res. Lett.*, **28**(1), 9–12, 2001.
- Chaigneau, A., *Variabilité de la température et salinité de surface à la traversée du courant Circumpolaire Antarctique au sud de l'Australie*. DEA Océan, Atmosphère, Environnement, Univ. Paul Sabatier, Toulouse, France, 2000.
- Gille, S. T., Mean sea surface height of the Antarctic Circumpolar Current from GEOSAT data: Method and application, *J. Geophys. Res.*, **99**, 18,255–18,273, 1994.
- Glowienka-Hense, R., GCM response to an Antarctic polyna, *Beitr. Phys. Atmos.*, **68**(4), 303–317, 1995.
- Gordon, A. L., Two stable modes of Southern Ocean winter stratification, in *Deep Convection and Water Mass Formation in the Ocean*, edited by J. Gascard and P. Chu, pp. 17–35, Elsevier Sci., New York, 1991.
- Levitus, S., *World Ocean Atlas 1998*, NOAA Atlas NESDIS, Natl. Oceanic and Atmos. Admin., Silver Springs, Md., 1998.
- Manabe, S., and R. J. Stouffer, Low-frequency variability of surface air temperature in a 1000-year integration of a coupled atmosphere–ocean–land surface model, *J. Clim.*, **9**, 5–23, 1996.
- McCartney, M., The subtropical recirculation of mode waters, *J. Mar. Res.*, **40**, 427–464, 1982.
- Moore, J. K., M. R. Abbott, and J. G. Richman, Location and dynamics of the Antarctic Polar Front from satellite sea surface temperature data, *J. Geophys. Res.*, **104**, 3059–3073, 1999.
- Morrow, R. A., R. Coleman, J. A. Church, and D. B. Chelton, Surface eddy momentum flux and velocity variances in the Southern Ocean from Geosat altimetry, *J. Phys. Oceanogr.*, **24**, 2050–2071, 1994.
- Nagata, Y., Y. Michida, and Y. Umimura, Variations of positions and structures of the ocean fronts in the Indian Ocean sector of the Southern Ocean in the period from 1965 to 1987, in *Antarctic Ocean and Resources Variability*, edited D. Salihage, pp. 92–98, Springer-Verlag, New York, 1988.
- Orsi, A. H., T. Whitworth III, and W. D. Nowlin, On the meridional extent and fronts of the Antarctic Circumpolar Current, *Deep Sea Res.*, **42**, 641–673, 1995.
- Reynolds, R. W., and D. C. Marsico, An improved real time global SST analysis, *J. Clim.*, **6**, 114–119, 1993.
- Rintoul, S. R., and J. L. Bullister, A late winter hydrographic section from Tasmania to Antarctica, *Deep Sea Res.*, **46**, 1417–1454, 1999.
- Rintoul, S. R., J.-R. Donguy, and D. H. Roemmich, Seasonal evolution of upper ocean thermal structure between Tasmania and Antarctica, *Deep Sea Res.*, **44**, 1185–1202, 1997.
- Rintoul, S. R., et al., Monitoring and understanding Southern Ocean variability and its impact on climate: A strategy for sustained observations, in *Recueil des actes: Le système d'observation de l'océan pour le climat*, *OceanObs 99*, St Raphaël, France, 1999.
- Russo, A., et al., Upper ocean thermal structure and fronts between New Zealand and the Ross Sea (austral summer 1994–1995 and 1995–1996), in *Oceanography of the Ross Sea, Antarctica*, Milan, Italy, 1999.
- Sarmiento, J. L., et al., Simulated response of the ocean carbon cycle to anthropogenic climate warming, *Nature*, **393**, 245–249, 1998.
- Sloyan, B. M., and S. R. Rintoul, The Southern Ocean limb of the deep overturning circulation, *J. Phys.*, **31**, 2001.
- Tchernia, P., Compte rendu préliminaire des observations océanographiques faites par le bâtiment polaire «Commandant CHARCOT» pendant la campagne 1949–1950, 1, *Bull. Inf. Compte Cent. Oceanogr. Etude Cotes*, **3**(1), 13–22, 1951a.
- Tchernia, P., Compte rendu préliminaire des observations océanographiques faites par le bâtiment polaire «Commandant CHARCOT» pendant la campagne 1949–1950, 2, *Bull. Inf. Compte Cent. Oceanogr. Etude Cotes*, **3**(2), 40–56, 1951b.
- Toole, J. M., Sea Ice, winter convection and the temperature minimum layer in the Southern Ocean, *J. Geophys. Res.*, **86**, 8037–8047, 1981.

A. Chaigneau and R. Morrow, Laboratoire des Etudes Géophysiques et Océanographiques Spatiales (LEGOS), UMR5566/GRGS, 18, av. Edouard Belin, 31401 Toulouse, Cedex 4, France. (Alexis.Chaigneau@cnes.fr; Rosemary.Morrow@cnes.fr)



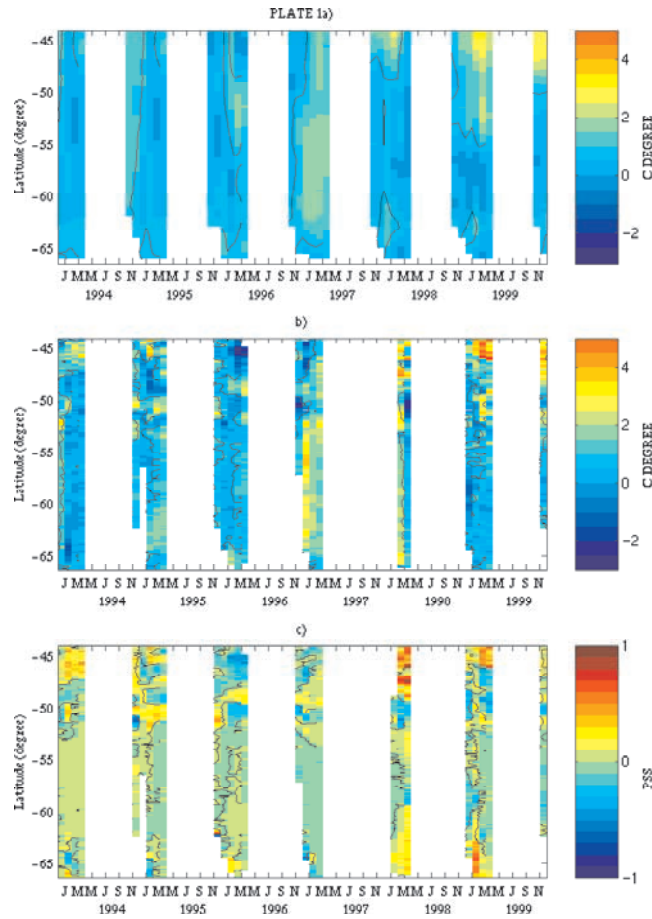


**Figure 6.** Hovmuller diagrams of a) Reynolds satellite SST anomalies, b) the thermosalinograph surface temperature anomalies. The monthly mean temperature calculated aver the 1993–1997 period is removed at each point along the line. c) The thermosalinograph surface salinity anomalies are calculated relative to the mean period 1993 to 1997: values for 1988 and 1999 are adjusted but not calibrated (see text for details).